Supporting Online Material for

The Contribution of Single Synapses to Sensory Representation in Vivo

Alexander Arenz, R. Angus Silver, Andreas T. Schaefer, Troy W. Margrie*

*To whom correspondence should be addressed. E-mail: t.margrie@ucl.ac.uk

This PDF file includes:

> Materials and Methods
> Figs. S1 to S3
> References

Other Supporting Online Material for this manuscript includes the following:
available at www.sciencemag.org/cgi/content/full/321/5891/977/DC1

> Movie S1

Supporting Online Material

Supplementary materials and methods

In vivo whole-cell recordings were carried out in freely breathing ketamine–xylazine anaesthetised (100 mg/kg–10 mg/kg) mice as previously described (*1*). Mice were head-fixed in the prone position and maintained at 35–37°C. Horizontal rotation was evoked using a custom-built motion device controlled by custom-written routines in Igor Pro. All recordings were performed in the dark during head-centred rotation about the earth vertical axis (yaw movement) using a compound sinusoidal positional command. Vestibular stimulation was discontinuous in that it consisted of repeated trials of a 5 s sinusoidal movement, separated by 2.5–4 s of baseline. Routinely, neurons were tested with movements of ± 20º amplitude at 0.3 Hz, confirmed with an accelerometer measuring three linear axes and three rotational axes mounted on the recording platform.

For recordings, a small craniotomy was performed in the petrosal bone to expose the pia mater. Granule cells were identified by their small capacitance ($\leq$ 5 pF) and high input resistance (0.6 ± 0.1 GΩ) (*2*), and were recorded at a depth of 1,180–1,660 μm from the surface. Granule cell EPSCs were recorded in voltage-clamp mode at −70 mV to isolate AMPA-mediated EPSCs (*3*), close to the reversal potential for chloride (*4,2*) to minimize the contribution of GABA receptor mediated events, using an internal solution containing (in mM; 130 methanesulfonic acid, 10 HEPES, 7 KCl, 0.05 EGTA, 2 Na_2ATP, 2 MgATP, 0.45 Na_2GTP plus 0.4% biocytin adjusted to pH 7.8 with KOH; 290 mOsm). EPSCs were detected using a 3−5 pA threshold criterion depending on recording noise, and subsequently confirmed by visual inspection. EPSCs were then aligned on the event onset and baselined over a 1 ms window ending 0.5 ms before the event. All recordings were carried out using an ADC/DAC board and a Power Mac computer running Igor Pro NClamp/Neuromatic for data acquisition. Signals were low-pass filtered at 8 kHz, digitized at 33.3 kHz and stored digitally for offline analysis.

The amplitude of EPSCs was determined by first detecting all EPSC waveforms with a minimum preceding inter-event interval of 5 ms. The peak current was taken as the single point maximum value that was then averaged across all events. Estimates for the weighted decay were calculated as the peak-normalized integral over 20 ms from EPSC onset. Therefore, the only EPSCs used were those in which a second event was not detected within 20 ms of EPSC onset. Coefficients of

variation (cvs) of EPSCs amplitudes were measured as the square root of the baseline-corrected variance at the peak of the average waveform of the onset-aligned EPSCs, divided by the average amplitude. Peri-stimulus time histograms (PSTHs) and charge transfer were calculated over 100 ms time bins from the onset time of events and the integral of the current trace, respectively. Putative MF recordings were carried out in current clamp and identified using criteria previously described (5). Significance of correlations was evaluated using Pearson's correlation coefficient (r). Statistical comparisons were carried out using either Student's t-test in cases of two data sets or analysis of variance (ANOVA). All values are given as average ± standard error of the mean (SEM).

For stimulus reconstruction, we followed a Bayesian approach as described in detail e.g. in (6) (7). In brief, Bayes' theorem states that the probability for a specific stimulus s after having measured a given response r (the "posterior distribution" $P(s|r)$ with r in our case being an m-dimensional vector of EPSC rates $r=\{r_1(t), r_2(t),...,r_m(t)\}$ and m being the number of inputs used for reconstruction, time dependence is generally omitted in this description for simplicity) is proportional to the likelihood $P(r|s)$, that is the likelihood to measure response r given the stimulus s, times the probability of stimulus s occurring at all ($P(s)$, the "prior" of the stimulus): $P(s|r)= P(r|s)*P(s) / P(r)$. A stimulus can now be reconstructed by maximizing this relation, thus determining the stimulus s' that has the highest probability to have evoked a given response r. The (marginal) normalizing probability $P(r)$ can be ignored if only the maximum of the probability distribution $P(s|r)$ is of interest, and thus only $P(r|s)$ and $P(s)$ need to be measured. Assuming independence of the n inputs, $P(r|s)$ can be factorized $P(r|s)= P(r_1|s) * P(r_2|s)....$ $*P(r_n|s)$. Each $P(r_i(t)|s)$ describes the EPSC rate distribution at time t in response to stimulus s. Assuming Poisson spiking statistics, $P(r_i|s)$ can be obtained directly from the neuron's tuning curve (average EPSC rate $f(s)$). The prior distribution $P(s)$ is measured from the applied velocity stimulus (black trace in Fig. 1c). To avoid floor and ceiling effects, Gaussian noise of 5°/s was added to the velocity trace before prior calculation.

One stimulus-evoked EPSC trial per cell was used for stimulus reconstruction. All remaining EPSC trials from all cells ($n–1$ per cell) were used to determine the tuning function $f(s)$ of average EPSC rates vs average velocity for a 100 ms time window sliding every 10 ms. As described above, for every time window the reconstructed stimulus ($s'(t)$) was identified as the stimulus with the highest probability ($P(s|r)$) of evoking the recorded response $r(t)$.

To determine the direction and velocity estimates for 1, 3, 8 and 12 synapses, individual EPSC trials from up to 12 different cells were used (for 12/18 cells a sufficient number of repetitions could be obtained to construct the tuning curve *f(s)*). For 100 synapses, cells were randomly sampled multiple times. The quality and reliability of the velocity estimates were quantified as the mean absolute difference between reconstructed stimulus and command stimulus and the standard deviation (SD) of this error, respectively, over 100 repetitions with different random seeds. We have assumed that the cells constituting the data set are independent of one another. If this is not correct then the calculated errors for a given number of synapses may increase due to potentially correlated noise in the input. All analysis was carried out in Igor Pro. Virtually identical results were obtained when a template-matching-based reconstruction algorithm was used (*6, 8*), where the reconstructed stimulus was determined based on highest correlation or shortest Euclidean distance.

Supplementary figures
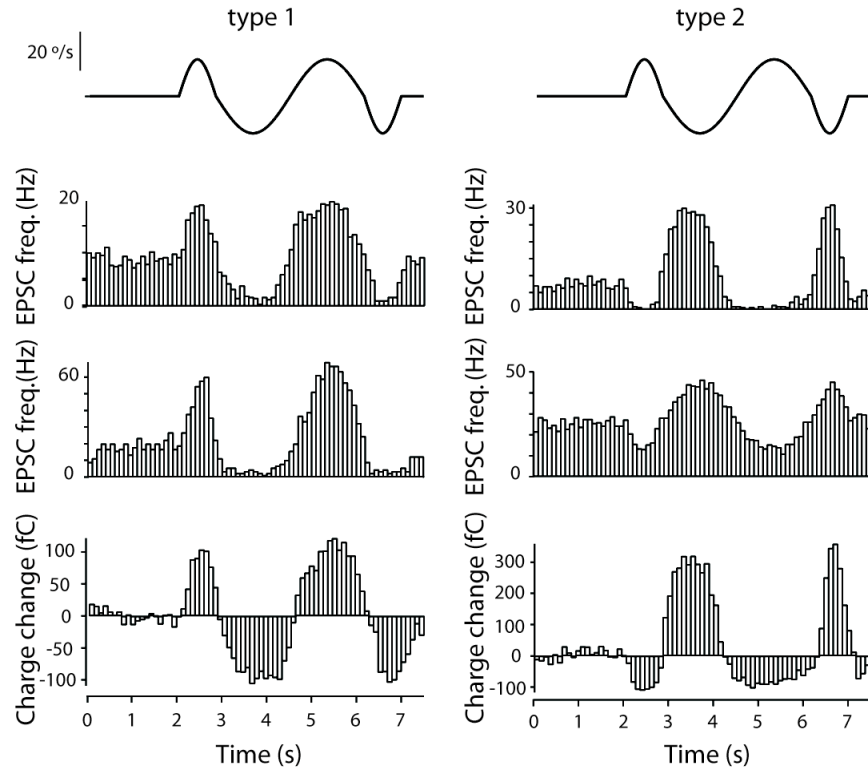
Fig. S1. Direction-sensitive EPSC rates reveal two types of responses. Top panels show the velocity waveform used to evoke the synaptic responses shown below. Example peri-stimulus time histograms (PSTHs) showing ipsilateral-preferring (type 1) and contralateral-preferring (type 2) responses. EPSC frequency (for four cells, top four PSTHs) and charge (for two cells, bottom two PSTHs) are plotted against time during stimulus presentation.
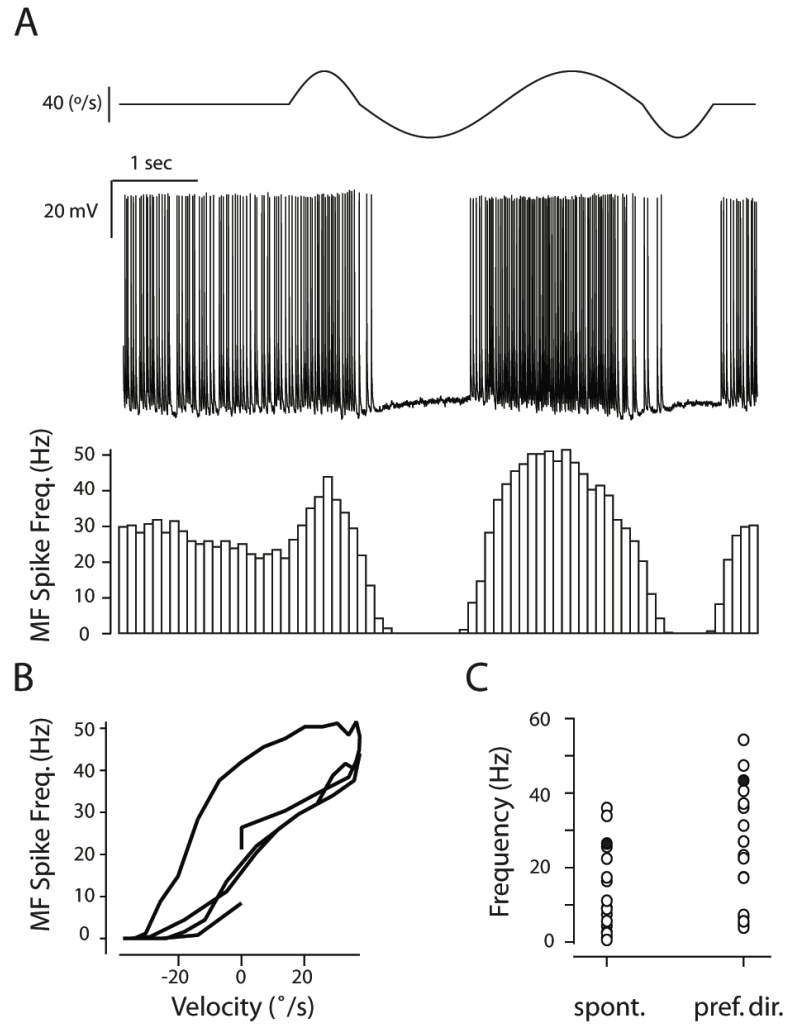
Fig. S2. Recording from a vestibular-sensitive putative MF terminal indicates high presynaptic firing rates. (**A**) Example trace of a MF bouton recording in current clamp (middle). (Below) The corresponding peri-stimulus time histogram generated from 25 stimulus repetitions showing the modulation of action potential frequency with respect to the velocity of motion (top trace). (**B**) MF action potential frequency plotted against the velocity of motion. (**C**) Population data comparing GC EPSC frequencies (open circles; n = 17) recorded during baseline and at a velocity of 30 °/s in the preferred direction to the frequency of MF discharge (filled circles; n = 1).
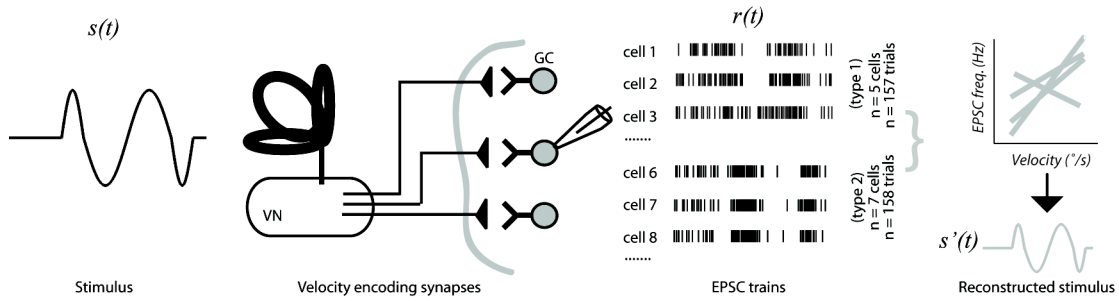
Fig. S3. Schematic illustrating the synapse-based Bayesian reconstruction approach. As a first step it is necessary to estimate from the EPSC data the probability of encountering the EPSC trial *r(t)* given the stimulus *s(t)*. Using Bayes' rule, this is combined with the prior distribution of stimuli *P(s)* to compute the posterior distribution *P(s|r)*. From this function, the stimulus *s'(t)* (which most probably evoked a given response *r(t)*) can be inferred. Individual EPSC trials from 12 cells in which we presented ten or more trials of a standardised stimulus were treated as individual vestibular encoding synapses and consisted of five type 1 and seven type 2 cells.

References

S1.   T. W. Margrie, M. Brecht, B. Sakmann, *Pflügers Archive - European Journal of Physiology* **444**, 491 (2002).

S2.   P. Chadderton, T. W. Margrie, M. Hausser, *Nature* **428**, 856 (2004).

S3.   L. Cathala, S. Brickley, S. Cull-Candy, M. Farrant, *J Neurosci* **23**, 6074 (2003).

S4.   S. G. Brickley, S. G. Cull-Candy, M. Farrant, *J Physiol* **497,** 753 (1996).

S5.   E. A. Rancz *et al.*, *Nature* **450**, 1245 (Dec 20, 2007).

S6.   K. Zhang, I. Ginzburg, B. L. McNaughton, T. J. Sejnowski, *J Neurophysiol* **79**, 1017 (1998).

S7.   A. Thiel, M. Greschner, C. W. Eurich, J. Ammermuller, J. Kretzberg, *J Neurophysiol* **98**, 2285 (2007).

S8.   A. T. Schaefer, K. Angelo, H. Spors, T. W. Margrie, *PLoS Biol* **4**, e163 (2006).